Article

Molecular Cell

Sequential Multisite Phospho-Regulation of KNL1-BUB3 Interfaces at Mitotic Kinetochores

Graphical Abstract

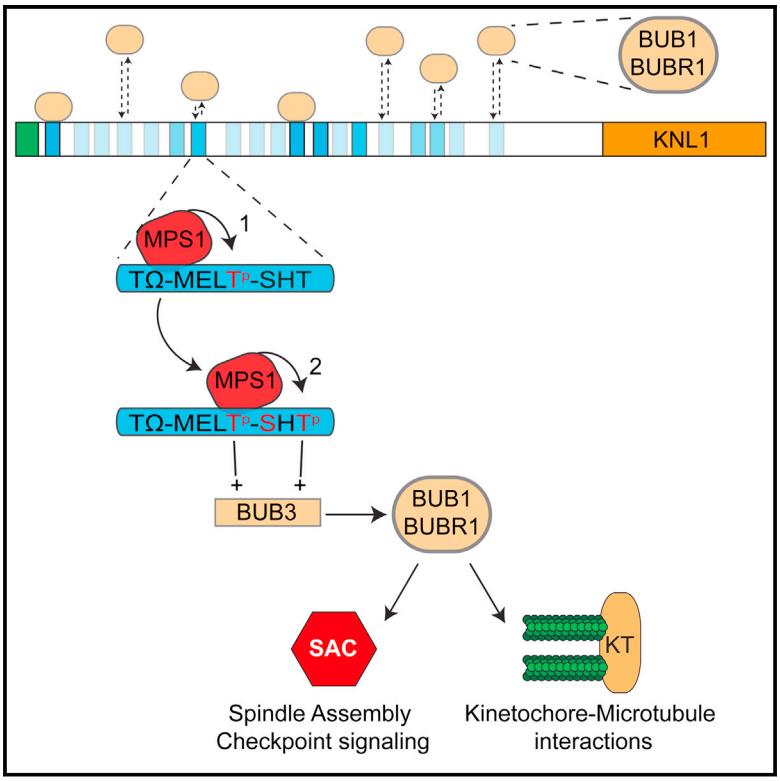

Highlights

- Systematic analyses of BUB kinetochore recruitment activity of KNL1 repeat sequences
- Active repeats are characterized by the presence of TΩ-MELT-SHT motifs
- MELT and SHT motifs are phosphorylated sequentially on Thr by the mitotic kinase MPS1
- A predicted SHpT-binding surface on BUB3 is required for its kinetochore localization

Authors

Mathijs Vleugel, Manja Omerzu, ..., Susanne M.A. Lens, Geert J.P.L. Kops

Correspondence

g.j.p.l.kops@umcutrecht.nl

In Brief

Short linear sequence repeats in the kinetochore scaffold KNL1 are required for error-free chromosome segregation by recruiting the BUB1/BUB3 kinase complex. Vleugel et al. report which repeats in human KNL1 are functional and define a human consensus sequence. They show that the kinase MPS1 sequentially phosphorylates two motifs within the consensus, creating a conserved and a vertebrate-specific binding site for BUB3.

Vleugel et al., 2015, Molecular Cell *57*, 824–835
March 5, 2015
http://dx.doi.org/10.1016/j.molcel.2014.12.036

CellPress

Molecular Cell
Article

Sequential Multisite Phospho-Regulation of KNL1-BUB3 Interfaces at Mitotic Kinetochores

Mathijs Vleugel,[1] Manja Omerzu,[1,2] Vincent Groenewold,[1,2] Michael A. Hadders,[1] Susanne M.A. Lens,[1] and Geert J.P.L. Kops[1,2,3,*]
[1]Molecular Cancer Research
[2]Department of Medical Oncology
[3]Cancer Genomics Netherlands
University Medical Center Utrecht, 3584 CG Utrecht, The Netherlands
*Correspondence: g.j.p.l.kops@umcutrecht.nl
http://dx.doi.org/10.1016/j.molcel.2014.12.036

SUMMARY

Regulated recruitment of the kinase-adaptor complex BUB1/BUB3 to kinetochores is crucial for correcting faulty chromosome-spindle attachments and for spindle assembly checkpoint (SAC) signaling. BUB1/BUB3 localizes to kinetochores by binding phosphorylated MELT motifs (MELpT) in the kinetochore scaffold KNL1. Human KNL1 has 19 repeats that contain a MELT-like sequence. The repeats are, however, larger than MELT, and repeat sequences can vary significantly. Using systematic screening, we show that only a limited number of repeats is "active." Repeat activity correlates with the presence of a vertebrate-specific SHT motif C-terminal to the MELT sequence. SHT motifs are phosphorylated by MPS1 in a manner that requires prior phosphorylation of MELT. Phospho-SHT (SHpT) synergizes with MELpT in BUB3/BUB1 binding in vitro and in cells, and human BUB3 mutated in a predicted SHpT-binding surface cannot localize to kinetochores. Our data show sequential multisite regulation of the KNL1-BUB1/BUB3 interaction and provide mechanistic insight into evolution of the KNL1-BUB3 interface.

INTRODUCTION

Large macromolecular assemblies called kinetochores coordinate the segregation of replicated chromosomes during mitosis. Kinetochores are essential for the formation of a physical link between centromeric DNA and microtubules of the mitotic spindle and are composed of more than 80 different proteins (Cheeseman and Desai, 2008; Foley and Kapoor, 2013). When kinetochores are not stably attached to microtubules, they activate a surveillance mechanism known as the spindle assembly checkpoint (SAC, or mitotic checkpoint) to prevent cell-cycle progression (Foley and Kapoor, 2013; Vleugel et al., 2012).

The outer kinetochore protein complex called the KMN network plays a central role in both the formation of stable kinetochore-microtubule attachments and SAC signaling (Sacristan and Kops, 2014; Cheeseman et al., 2006; Foley and Kapoor, 2013; Kiyomitsu et al., 2007). It is a ten-subunit network assembled from three subcomplexes, *K*NL1-C, *M*IS12-C, and *N*DC80-C. The largest protein in the network, the scaffold KNL1 (also referred to as CASC5/AF15q14/Blinkin), directly interacts with microtubules using a basic patch near its N terminus and is incorporated into the KMN network by virtue of its C-terminal RWD domains (Kiyomitsu et al., 2007; Petrovic et al., 2014; Welburn et al., 2010). The N-terminal half (~1,200 amino acids) of KNL1 is an assembly hub for protein complexes involved in SAC signaling and attachment-error correction. Via a multitude of so-called MELT motifs, KNL1 recruits BUB3, BUB1, and BUBR1 to unattached kinetochores (Krenn et al., 2014; London et al., 2012; Shepperd et al., 2012; Vleugel et al., 2013; Yamagishi et al., 2012; Zhang et al., 2014). These "BUB proteins" are members of the original set of SAC components identified in yeast genetic screens (Hoyt et al., 1991; Li and Murray, 1991). Both BUB1 and BUBR1 heterodimerize with BUB3 and may additionally form higher-order assemblies with each other (Larsen et al., 2007; Taylor et al., 1998). Besides regulating SAC signaling, they impact on error correction by regulating Aurora B kinase localization or phosphorylation of its targets. BUB1 kinase activity, for example, ensures proper inner-centromere localization of Aurora B (Kawashima et al., 2009), while BUBR1—via recruitment of the PP2A-B56 phosphatase—dampens excessive Aurora B activity by dephosphorylating its substrates within the KMN network (Foley et al., 2011; Kruse et al., 2013; Suijkerbuijk et al., 2012b; Xu et al., 2013). Finally, KNL1 recruits the PP1 phosphatase via N-terminally located SILK/RVSF motifs (Liu et al., 2010). Kinetochore localization of PP1 aids stabilization of kinetochore-microtubule attachments and promotes SAC silencing in metaphase (Nijenhuis et al., 2014; Liu et al., 2010; Meadows et al., 2011; Rosenberg et al., 2011).

Kinetochore binding of the BUBs and PP1 is regulated by phosphorylation. While the KNL1-PP1 interaction is disrupted by Aurora B-dependent phosphorylation of the SILK/RVSF motifs (Liu et al., 2010), the KNL1-BUB interaction is promoted by MPS1-dependent phosphorylation of the MELT-like sequences in KNL1 (London et al., 2012; Shepperd et al., 2012; Yamagishi et al., 2012). The methionine and phospho-threonine of the MELpT sequence dock onto a hydrophobic and basic pocket, respectively, of the BUB3 subunit of the BUB3/BUB1 dimer (Primorac et al., 2013). The total number and primary sequence

identity of the MELT-like motifs in KNL1 homologs varies greatly among different organisms (Vleugel et al., 2012, 2013). Human KNL1, for example, contains an array of 19 repeat modules with variations of a TxxΩ-(Xn)-MELT sequence, in which the TxxΩ contributes critically to BUB1 localization by an unknown mechanism (Vleugel et al., 2013). The repeating units, however, extend beyond the TΩ and MELT motifs, but the relevance of these additional sequences for KNL1 function is unknown. All 19 repeat modules in human KNL1 might cooperate to recruit sufficient levels of BUB proteins to unattached kinetochores (Krenn et al., 2014; Vleugel et al., 2013; Zhang et al., 2014), but some diverge more strongly from the consensus sequence than others, and some lack essential residues in the TxxΩ or MELT motifs (Vleugel et al., 2012, 2013). In fact, some repeats are interchangeable, and KNL1 function is supported by an engineered array containing six copies of a single functional repeat (Vleugel et al., 2013).

Here we set out to systematically decipher the molecular requirements for the KNL1-BUB interfaces by determining the functionality of each individual repeat unit in KNL1. We show that the "active" repeats in human KNL1 contain a "SHT" motif C-terminal to the MELT that is phosphorylated by MPS1 in a manner that requires prior MELT phosphorylation. SHpT contributes essential contacts with basic residues in BUB3, and both are indispensable for efficient BUB1/BUB3 localization and chromosome biorientation. Our data suggest that human KNL1 repeats have evolved to extend the electrostatic interface with BUB3, providing a framework for understanding the rapid evolution of the KNL1-BUB interface.

RESULTS

Systematic Dissection of KNL1 Repeat Functionality

Human KNL1 has 19 repeating units (see Figure 1C for schematic representation). We and others previously showed that KNL1 does not require the full complement of repeats to recruit BUB1 to kinetochores (Vleugel et al., 2013; Zhang et al., 2014) and that not all repeats are equally proficient in doing so. For example, while six copies of repeat 17 could functionally replace the full array of 19 repeating units, six copies of repeat 2 could not (Vleugel et al., 2013). To examine if in vivo functionality of the repeats corresponds to affinity for the BUB3/BUB1 dimer, we reconstituted KNL1-BUB binding in vitro using the His_6-$BUB1^{1-280}$/BUB3 complex (Krenn et al., 2014) and various GST-tagged KNL1 fragments (Figure 1A). These included a fragment containing repeats 12–14 (KNL1-M_3; Vleugel et al., 2013), a non-functional variant thereof (KNL1-A_3, harboring four alanine substitutions at the TxxΩ-MxxT positions), and two engineered fragments with three copies of either repeat 2 or 17 (KNL1-2_3 and KNL1-17_3; Vleugel et al., 2013). All GST-KNL1 proteins were pre-phosphorylated in vitro by recombinant MPS1. Whereas $BUB1^{1-280}$/BUB3 efficiently co-purified with KNL1-M_3 and KNL1-17_3, binding of KNL1-2_3 was weak, and virtually no binding was detected for KNL1-A_3 (Figure 1B). Thus, the correlation between interaction with BUB1/BUB3 and in vivo functionality implies that the role of the repeat sequences in mitosis is restricted to BUB1/BUB3 binding.

To systematically assess functionality of individual repeats, we used the previously published LAP-tagged $KNL1^{\Delta}$ protein (KNL-N^{1-86} fused to KNL-$C^{1833-2432}$) that is devoid of repeat units but maintains PP1- and microtubule-binding and kinetochore localization (Vleugel et al., 2013). Into this $KNL1^{\Delta}$ we inserted engineered variants of the KNL1-M_3 fragment in which repeats 12–14 were each replaced with identical copies of one of the 19 repeats. All non-repeat sequences of the 223-amino acid M_3 fragment were left intact. This generated 19 variants: $KNL1^{\Delta}$-1_3, $KNL1^{\Delta}$-2_3, and so forth, up to $KNL1^{\Delta}$-19_3 (Figure 1C). These engineered KNL1 proteins were expressed from a doxycycline-inducible promotor at a single integration site in HeLa cells and assessed for their ability to functionally replace endogenous KNL1 (Vleugel et al., 2013). KNL1-FL (full-length), $KNL1^{\Delta}$, and $KNL1^{\Delta}$-A_3 were used as controls (Vleugel et al., 2013). We first tested the ability of all KNL1 variants to recruit BUB1 to unattached kinetochores. Since each engineered fragment contains three copies of an individual repeat and repeats function independently (Vleugel et al., 2013), we divided the observed BUB1 kinetochore intensities by three to reflect the BUB1 recruitment potential of individual repeats. As shown in Figure 1D, the various engineered KNL1 variant proteins restored BUB1 kinetochore localization to different extents (see also Figures S1A and S1B). BUBR1 kinetochore levels followed a similar pattern (Figures S1A and S1B), in agreement with an essential role for BUB1 in BUBR1 kinetochore localization. We classified the BUB1 recruitment ability of individual repeats as "high" (repeats 1, 11, and 12; green bars), as "low" (repeats 2–5, 8–10, 13, 15, 16, 18, and 19; absent or red bars), and the remaining repeats as "intermediate" (repeats 6, 7, 14, and 17; yellow bars). Combined, the amount of BUB1 recruited to kinetochores by the 19 repeats added up to similar amounts as recruited by full-length KNL1 (Figure 1D), verifying that the repeats function as autonomous BUB recruitment modules and that BUB1 recruitment ability of KNL1 is provided solely by the 19 repeats.

Nocodazole-treated cells depleted of KNL1 are unable to sustain a mitotic arrest in the presence of low doses of the MPS1 inhibitor reversine (250 nM) (Santaguida et al., 2011; Saurin et al., 2011; Vleugel et al., 2013). The ability of the engineered KNL1 variants to support SAC signaling showed a bimodal distribution and correlated strongly with BUB1 recruitment potential. All repeats classified as "high" in BUB1 recruitment were able to restore SAC activity (Figure 1E; green curves). In contrast, repeats classified as "low" could not restore SAC activity (red curves), while the "intermediate" ones (yellow curves) were either SAC proficient or SAC deficient (Figure 1E). The efficiency of chromosome alignment quantitatively tracked kinetochore BUB1 levels (Figure S2A), as we previously showed for a subset of the repeats (Vleugel et al., 2013). Thus, whereas chromosome alignment efficiency follows the amount of BUB1 recruited by KNL1, the SAC appears to rely on an amount of BUB1 above some (albeit low) threshold (Figure 1F). This raises the question of how many molecules of BUB1 are bound by a single molecule of KNL1 at steady state. To estimate this, we replaced endogenous BUB1 or KNL1 with LAP-tagged, siRNA-resistant, full-length versions and quantified how much LAP-BUB1 or LAP-KNL1 was required for restoring a comparable amount of BUB1 to unattached kinetochores (Figures 1G and 1H;

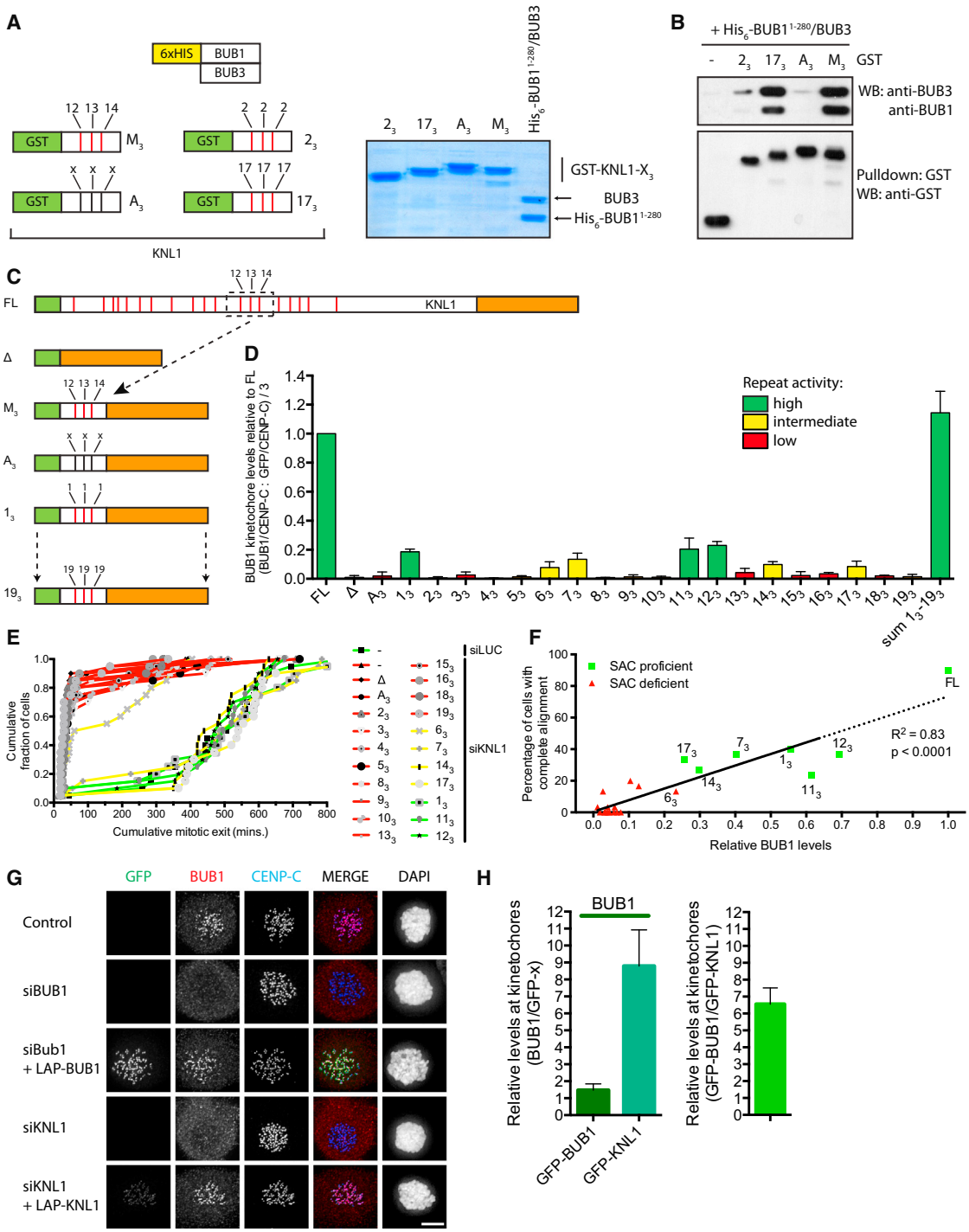

Figure 1. Systematic Functional Characterization of Human KNL1 Repeats

(A) Schematic representation (left) and Coomassie-stained SDS-PAGE (right) of recombinant GST-KNL1 variants and the His_6-BUB1$^{1-280}$/BUB3 complex. Red stripes in schematic represent repeat sequences.

(B) Immunoblots of BUB1, BUB3, and GST from in vitro binding assays of GST-KNL1 with His_6-BUB1$^{1-280}$/BUB3. GST-tagged KNL1-M_3 variants were pre-phosphorylated by 50 ng MPS1 (1 hr at 30°C), coupled to glutathione-agarose beads and incubated with His_6-BUB1$^{1-280}$/BUB3 dimers for 1 hr. Western blots are representative of three experiments.

(C) Schematic representation of KNL1-FL, KNL1$^{\Delta}$, KNL1$^{\Delta}$-M_3, and its derivatives.

(D) Quantification of BUB1 kinetochore signal intensity in Flp-in HeLa cells expressing the indicated LAP-KNL1 variants. Intensity of BUB1 is corrected for LAP-KNL1 and CENP-C levels, divided by three, and depicted as relative to that of cells expressing full-length LAP-KNL1. Error bars show SEM of three experiments. The asterisk denotes the sum of values of BUB1 levels of all repeats.

(legend continued on next page)

Figure S2B; see Experimental Procedures for technical details). As depicted in Figure 1H, 6.56 (±0.96) times more LAP-BUB1 than LAP-KNL1 was required to achieve the same level of kinetochore BUB1, suggesting that at steady state in a nocodazole-treated mitotic cell, one KNL1 molecule is bound by, on average, 6–7 BUB1 molecules. This ratio roughly corresponded to the BUB1:KNL1 ratio measured in prometaphase (Figures S2C and S2D).

Dissecting Common Characteristics of "Active" KNL1 Repeats

In general, eukaryotic KNL1 homologs strongly diverge in the number and sequence of their repeats (Vleugel et al., 2012, 2013). Due to the rapidly evolving nature of KNL1, we were unable to generate a sequence alignment of distant KNL1 orthologs. We could, however, make a primary sequence alignment of a number of placental mammalian homologs in which the MELT-containing repeats were relatively easily identified (Table S1). We observed that many of these repeats have degenerated from the consensus repeat sequence (Figure S3). When comparing the sequence logo of all 19 repeats (Vleugel et al., 2013) to a weighted sequence logo based on the functionality of each repeat, enrichment of specific sequences became apparent (Figures 2A and 2B). Activity of the repeats correlated to the following "consensus" sequence: DKTΦΦΩS[ED]x[ED]$_{2\text{-}3}$xxM[DE]ΦTxSHTΦxΦ (where x denotes any amino acid and Φ and Ω denote hydrophobic and aromatic residues, respectively) (Figure 2B).

In order to uncover functional motifs/residues in active repeats, we made use of KNL1-NC, a 261 residue, N-terminal fragment of KNL1 fused to the C-terminal kinetochore-targeting region. KNL1-NC contains only a single repeat (encompassing the active repeat 1 accompanied by the two KI motifs) and is sufficient for SAC function (Krenn et al., 2014; Vleugel et al., 2013). Various residues of repeat 1 within KNL1-NC were systematically mutated (Figure 2C), and the ability of mutant KNL1-NC to activate the SAC and recruit BUB1 activity (as measured by H2AT120P signal; Kitajima et al., 2005) was examined. As predicted from the *Saccharomyces cerevisiae* Bub3/Bub1-MELpT structure (Primorac et al., 2013), mutating the methionine (M177A; NC^{ADLT}), aspartate (D178K; NC^{MKLT}), or threonine (T180A; NC^{MDLA}) of the MDLT motif in repeat 1 abolished SAC activity (Figures 2C and 2D), but significant kinetochore BUB1 activity remained in the NC^{MKLT} and NC^{MDLA} mutants (Figure 2E). Interestingly, repeat 1 diverges from the consensus "active" sequences due to the presence of a serine following the MDLT motif, instead of a lysine (Figures 2B and 2C). Substituting this serine for lysine (S181K; NC^{S181K}) enhanced the BUB1 recruitment ability of repeat 1 3-fold, as judged by increased levels of BUB1 and H2AT120 phosphorylation (Figures S5A and S5B; Figures 2C and 2E). These analyses further showed that changing a hydrophobic residue in the TΩ motif to an acidic residue (V169E; NC^{V169E}) abolished repeat function (Figures 2C and 2D).

Importantly, mutational dissection of repeat 1 showed that the previously uncharacterized SHT motif, located C-terminally to the MDLT motif, was required for SAC activity and H2AT120 phosphorylation (NC$^{SHT\text{-}AAA}$ in Figures 2C–2E). To examine the importance of this motif, we sought to restore the SHT sequence in a repeat in which the SHT motif was absent. Repeat 16 closely adheres to the consensus "high activity" sequence, with the exception of the SHT motif that in repeat 16 has the sequence SCM (Figure S3). Repeat 16 was classified in our analyses as "inactive" (Figures 1D–1F). Substituting SCM for SHT in the KNL1$^{\Delta}$-16$_3$ protein (creating KNL1$^{\Delta}$-16$_3^{SHT}$) enhanced BUB1 levels at kinetochores 2-fold (Figures 2F and 2G), showing that the SHT motif indeed is an important determinant of BUB kinetochore recruitment in human cells.

KNL1 Repeats Are Phosphorylated on Multiple Sites by MPS1

The sequence logo of the "high" activity repeats showed that five threonines and serines were strongly represented, including the one in the MELT motif, the two in the SHT motif, and two in the TxxΩS motif (Figure 2B). We therefore hypothesized that in addition to the MELT motif, phosphorylation of other residues in the repeat affect the interaction with BUB1/BUB3. In support of this, a mutant KNL1-M$_3$ protein that contained alanine substitutions for the threonines in the three MELT motifs (KNL1-M$_3^{MELA}$) could be phosphorylated in vitro by recombinant MPS1 (Figure 3A), and this still enhanced in vitro binding of KNL1-M$_3^{MELA}$ to BUB3/BUB1 (Figure 3B). Moreover, cells expressing KNL1$^{\Delta}$-M$_3^{MELA}$ were able to recruit significant amounts of BUB1 to kinetochores (Figures S5C and S5D). Together, these data suggest that next to the phosphorylation of MELT motifs, phosphorylation of other sequences is involved in regulating the KNL1-BUB3/BUB1 interaction. Mass spectrometric analyses of KNL1-M$_3$ and KNL1-17$_3$ proteins in vitro phosphorylated by MPS1 identified phosphoresidues in the MELT, TΩ, and SHT motifs of repeat 12 and repeat 17 (Figure 3C; Figures S4A and S4B). Furthermore, similar analyses of immunoprecipitated LAP-KNL1-FL from nocodazole-arrested cells identified phosphoresidues in the MDIT and SHT motifs of repeat 7 (Figure 3D; Figure S4C). We suspect that low coverage and low occupancy prevented us from identifying phosphorylation of other repeats. We do note, however, that large-scale phospho-proteomics

(E) Time-lapse analysis of Flp-in HeLa cells expressing LAP-KNL1 variants, transfected with siLUC or siKNL1, and treated with nocodazole and 250 nM reversine. Data (n = 40, representative of three independent experiments shown) indicate cumulative fraction of cells that exit from mitosis (as scored by cell morphology using DIC) at the indicated time after NEB. Colors denote high (green curves), intermediate (yellow curves), and low (red curves) active repeats as judged by BUB1 localization in Figure 1D.

(F) Percentage of cells with complete chromosome alignment after 45 min treatment with MG132 plotted against the relative BUB1 kinetochore levels for each KNL1 variant. Green squares denote SAC-proficient repeats; red triangles denote SAC-deficient repeats.

(G and H) Representative images (G) and quantification (Figure S2B) of GFP levels at kinetochores of HeLa cells expressing LAP-BUB1 or LAP-KNL1, transfected with siRNAs to luciferase (siLUC), BUB1 (siBUB1), or KNL1 (siKNL1) and treated with nocodazole. Bars, 5 μm. Graph in (H) displays total kinetochore signal intensities (+SD) of BUB1(/CENP-C) as a ratio of LAP-BUB1(/CENP-C) or LAP-KNL1(/CENP-C). Data are from 40 cells (representative of three experiments). Right graph shows the ratio of BUB1(/CENP-C)/LAP-BUB1(/CENP-C) over BUB1(/CENP-C)/LAP-KNL1(/CENP-C) (three experiments, +SD).

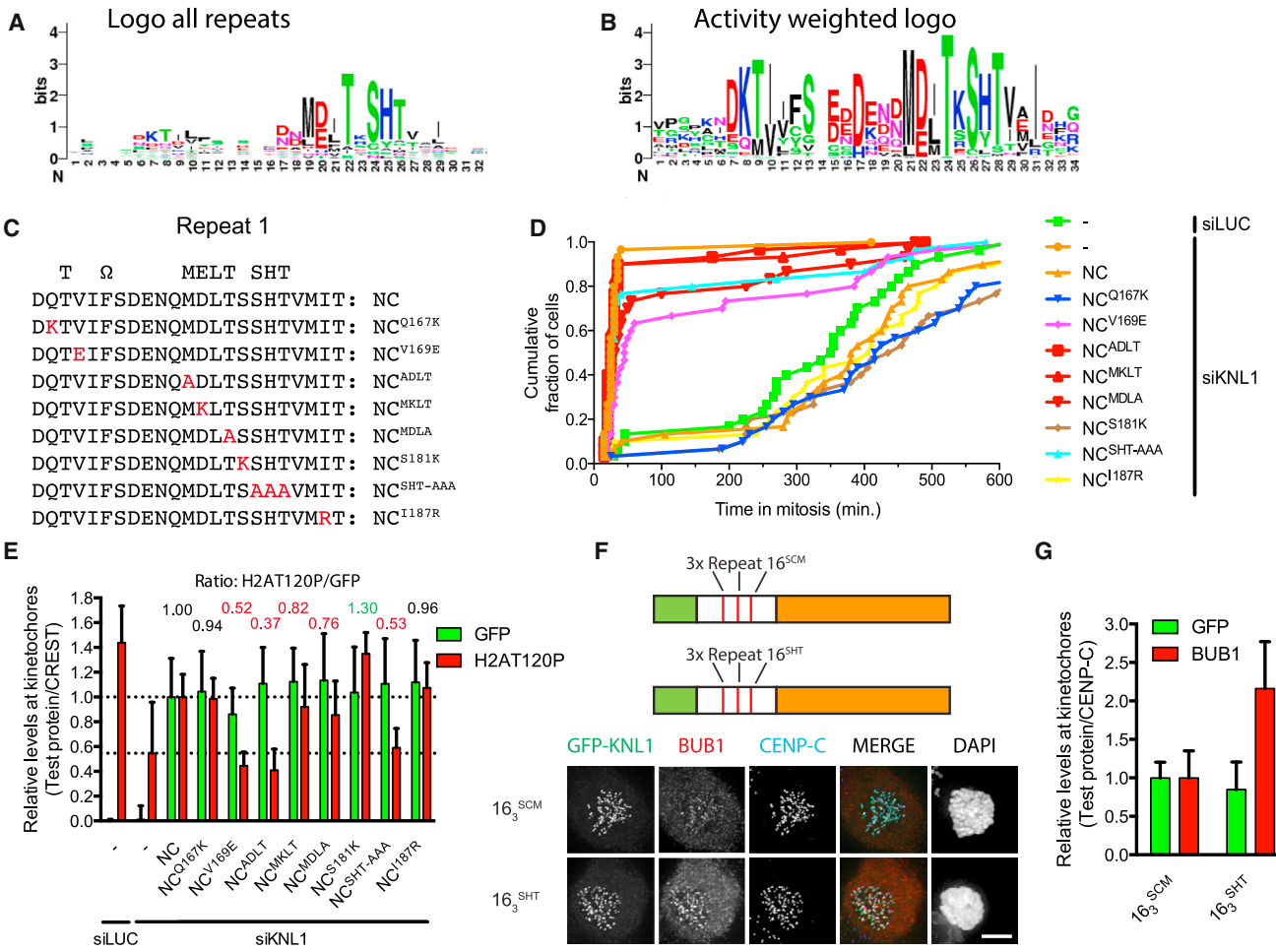

Figure 2. Identification of Common Characteristics of "Active" KNL1 Repeats

(A and B) Sequence logo of all repeats of human KNL1 (A) and a weighted sequence logo (B) based on functionality of each repeat, where each % of contribution of the repeat to full BUB1 recruitment (Figure 1D) corresponded to the amount of times that repeat was added to the multiple sequence alignment and subsequent logo analysis (e.g., repeat 1 contributes ~18% to BUB1 kinetochore levels and its sequence was added 18 times to the analysis, etc.).

(C) Schematic representation of LAP-KNL1-$N^{1\text{-}261}$-$C^{1833\text{-}2342}$ protein variants with mutations in repeat 1.

(D) Time-lapse analysis of Flp-in HeLa cells expressing LAP-KNL1-NC variants, transfected with siLUC or siKNL1, and treated with nocodazole and 250 nM reversine. Data (n = 40, representative of three independent experiments shown) indicate cumulative fraction of cells that exit from mitosis (as scored by cell morphology using DIC) at the indicated time after NEB.

(E) Quantification of H2AT120P/CREST and GFP/CREST in cells expressing various LAP-tagged KNL1-NC mutants treated with nocodazole. Ratios of normalized H2AT120P:GFP (+SD) are indicated for each KNL1-NC variant.

(F and G) Representative images (F) and quantification (G) of GFP and BUB1 kinetochore levels in nocodazole-treated cells expressing $KNL1^{\Delta}$-$16_3{}^{SCM}$ or $KNL1^{\Delta}$-$16_3{}^{SHT}$ (schematically depicted in upper panel). Bars, 5 μm. Graph in (G) displays total kinetochore signal intensities (+SD) of LAP-KNL1 and BUB proteins over CENP-C. Data are from 15 cells and representative of three experiments. Levels of kinetochore LAP-KNL1 and BUB1 were set to 1 in $KNL1^{\Delta}$-$16_3{}^{SCM}$-expressing cells.

studies have also reported phosphorylation of MDIT and SHT of repeat 7 of human KNL1 (Dephoure et al., 2008; Grosstessner-Hain et al., 2011; Hegemann et al., 2011).

Multisite Phosphorylation of KNL1 Repeats by MPS1 Controls BUB1/BUB3 Binding

To assess the functional relevance of the phosphorylated residues, we tested in vitro binding of BUB3/BUB1 to variants of GST-KNL1-M_3 (Figure S5E) in which the phosphoresidues were substituted for alanines (Figure 3E). Whereas KNL1-M_3 showed a strong interaction with BUB1/BUB3, mutations in either the MELT (KNL1-$M_3{}^{MELA}$) or SHT (KNL1-$M_3{}^{AHA}$) motifs greatly decreased binding (Figures 3F and 3G). In contrast, mutation of the TxxΩS motif (KNL1-$M_3{}^{A\Omega A}$) did not affect the interaction with BUB1/BUB3. Combining mutations in the MELT and SHT motifs (KNL1-$M_3{}^{MELA\text{-}AHA}$) or in all three motifs (KNL1-$M_3{}^{5A}$) completely abolished BUB3/BUB1 binding (Figures 3F and 3G). The ability of the KNL1-M_3 variants to bind BUB3/BUB1 in vitro strongly correlated with their ability to recruit BUB1 to kinetochores and to support SAC signaling

(Figures 3H–3J). Together, these data show that multisite phosphorylation of the MELT and SHT motifs in KNL1 repeats by MPS1 synergizes to regulate the KNL1-BUB interface.

SAC activation and chromosome alignment require different activity levels of KNL1 repeats (Figure 1F). To test whether multisite phosphorylation on MELT and SHT motifs differentiates between these two activities, we made use of our previously described KNL1 variant containing six repeats (KNL1$^{\Delta}$-M_3-M_3), which completely rescues BUB1 kinetochore localization, chromosome alignment, and the SAC (Vleugel et al., 2013). Mutation of all SHT phosphorylation sites (KNL1$^{\Delta}$-M_3^{AHA}-M_3^{AHA}) strongly reduced but did not abolish BUB1 kinetochore levels (Figures S5F and S5G). In contrast to the KNL1 variant containing three mutant SHT motifs (KNL1$^{\Delta}$-M_3^{AHA}) (Figure 3J), the BUB1 levels recruited by KNL1$^{\Delta}$-M_3^{AHA}-M_3^{AHA} now exceeded the threshold required to promote SAC activity (Figure S5I), showing that MELT phosphorylation is sufficient to maintain the SAC. Unlike its ability to support the SAC, expression of KNL1$^{\Delta}$-M_3^{AHA}-M_3^{AHA} strongly impaired chromosome alignment (Figure S5H). In human cells, therefore, SHT phosphorylation provides a critical contribution to this function of KNL1. Since the SHT motif most likely arose after the MELT motifs, expanding the repeats to include the SHT motifs during evolution may have permitted increased kinetochore BUB levels and thereby promoted kinetochore-microtubule attachment and biorientation in higher vertebrates.

Sequential Phosphorylation of MPS1 Sites within KNL1 Repeats

To assess repeat phosphorylation in cells, we generated phospho-specific antibodies to detect MELpT and SHpT sequences. Antibodies generated against phospho-peptides containing MEIpT of repeat 13/17 (pT943/pT1155) and SHpT of repeat 8 (pT605) recognized unattached kinetochores, and the signals were dependent on the presence of KNL1 and on MPS1 kinase activity (Figures 4A–4D). Although classified as "inactive" (Figure 1D), repeat 8 is phosphorylated on its SHT motif in vivo, suggesting that BUB recruitment by this repeat is hampered by mutations that do not affect its phosphorylation by MPS1.

MPS1 prefers to phosphorylate threonines preceded by an acidic residue (D/E) at position −2, −3, or −4 (Dou et al., 2011; Hennrich et al., 2013; Jelluma et al., 2008) and followed by a hydrophobic amino acid (I, L, or V) at position +3 (Hennrich et al., 2013). Interestingly, SHT motifs are often followed by I/L at +3 (Figure 2B), and prior phosphorylation of either the serine of SHT (−2) and/or the threonine of MELT (−4) could contribute the necessary negative charges, perhaps even sequentially (first position −4 [MELpTxSHT], then −2 [MELpTxpSHT], then 0 [MELpTxpSHpT]). To test the hypothesis that MPS1 can prime its own substrate recognition sites within KNL1 repeats we examined if phosphorylation of SHT relies on prior phosphorylation of MELT. The ability of MPS1 to establish repeat phosphorylations was assessed using our phospho-specific antibodies on nocodazole-treated cells in which MPS1 was activated by washout of reversine. Indeed, expression of KNL1$^{\Delta}$-8_3 carrying alanine substitutions of the threonines of all three MDLT motifs (KNL1$^{\Delta}$-8_3^{MDLA}) strongly reduced kinetochore signals of the SHpT antibody following MPS1 reactivation (Figure 4E). In contrast, MEIT phosphorylation of repeat 13/17 was independent of SHT phosphorylation (Figure 4F). Since epitope recognition by the SHpT antibody was not affected by mutating the MEIT motif (Figure S5J), we conclude that phosphorylation of the MELT motifs aids subsequent phosphorylation of the SHT motif to establish multisite regulation of the KNL1 repeats.

A Basic Patch on Human BUB3 Interacts with Phosphorylated SHT Motifs

Electrostatic interactions between MELpT and ScBub3 contribute to Bub3 localization and SAC activity in budding yeast (Primorac et al., 2013). Since our data show that interaction of human KNL1 with BUB1/BUB3 is stimulated by multisite phosphorylation of the repeats in KNL1, we hypothesized that phosphorylated SHT motifs may interact with a basic patch in BUB3 that is distinct from the one interacting with MELpT. Based on the structure of ScBub3-MEMpT (Primorac et al., 2013) (Figure 5A), we generated a homology model of human BUB3 on which we superimposed the budding yeast MEMpT-peptide (purple) and BUB1$^{289-359}$ (cyan) (Figure 5B). In contrast to yeast Bub3, human BUB3 has an extended basic surface in the vicinity of the predicted location of the phosphorylated SHT motif (Figures 5A and 5B, bottom panels). Importantly, some of the residues that create this extended basic path (R157/R158 and R173/R174) are present in the human BUB3 but not in the *S. cerevisiae* ortholog (Figure 5C), corresponding to the presence of a SHT motif in repeats of human but not *S. cerevisiae* KNL1 (Vleugel et al., 2013). We produced recombinant BUB3 proteins with charge-reversal mutation of the basic patches predicted to interact with SHpT. Some mutants could not be further analyzed because of diminished protein stability and BUB1 binding, but BUB3$^{173E/174E}$ was expressed and purified as a stable dimer with BUB1 (Figure S5K). In contrast to wild-type BUB3, this mutant was incapable of binding to KNL1-M_3 in vitro (Figure 5D) and did not localize to kinetochores (Figure 5E). This supports the hypothesis that the extended basic surface in human BUB3 is required for interaction with SHpT.

Together, these results show that human KNL1 repeat sequences are sequentially phosphorylated by MPS1 to provide interaction surfaces for basic patches in BUB3.

DISCUSSION

The KNL1-BUB3 Interfaces

We show that only a limited number of the 19 repeats in human KNL1 are active and that the ability to recruit BUB1 to unattached kinetochores varies strongly between repeats (Figure 6). These differences can be linked to various degrees of degeneration of repeat sequences from the consensus "active" sequence. For example, degeneration of TΩ is likely to explain inactivity of repeats 3, 8, 13, and 15, while degeneration of two motifs is likely to have inactivated repeats 2, 10 (MELT and TΩ), and 9 (MELT and SHT). Especially striking are repeats 5 and 19 that have lost all three motifs. Repeat 18 is interesting in this respect because it is inactive but appears to adhere closely to the "active" sequence. Perhaps it suffers from a combination of slightly less well-tolerated substitutions such as the valine and aspartate directly surrounding the threonine of the

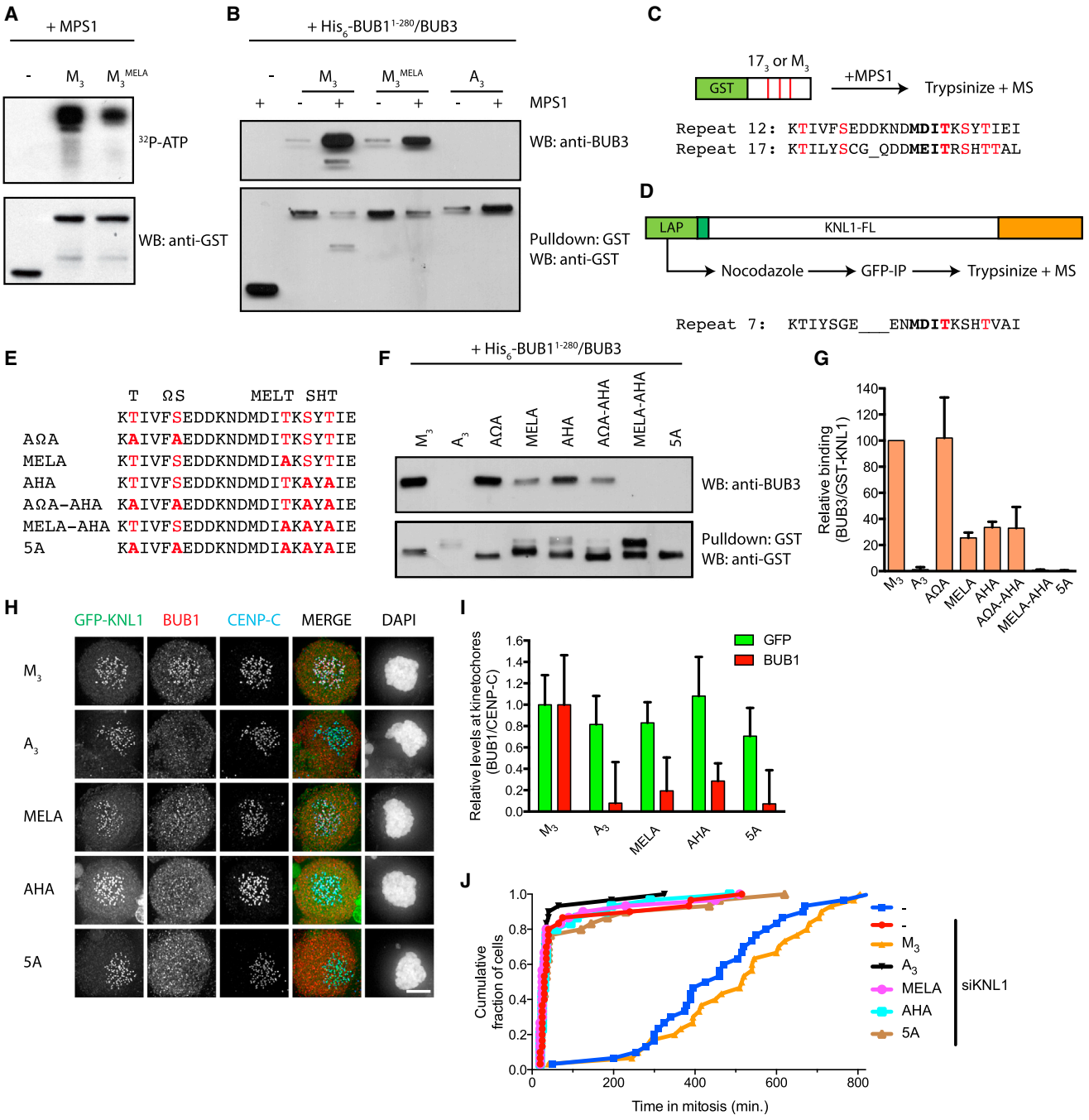

Figure 3. Multisite Phosphorylation of KNL1 Repeats Is Essential for Efficient BUB1/BUB3 Binding

(A) Radiograph (upper) and immunoblot (lower) of in vitro MPS1 kinase assay using GST (–), GST-KNL1-M_3, or GST-KNL1-M_3^{MELA} as substrates.

(B) Immunoblots of BUB1, BUB3, and GST from in vitro binding assays of GST-KNL1 with His_6-$BUB1^{1-280}$/BUB3. GST-tagged KNL1-M_3 variants were pre-phosphorylated by 50 ng MPS1 (1 hr at 30°C) wherever indicated (+), coupled to glutathione-agarose beads and incubated with His_6-$BUB1^{1-280}$/BUB3 dimers for 1 hr. Western blots are representative of three experiments.

(C and D) Schematic representations of experimental setups and sequences of identified phosphopeptides from GST-KNL1 variants in vitro phosphorylated by MPS1 (C) or from LAP-KNL1 immunoprecipitation from nocodazole-treated cells (D). Phosphorylated residues are depicted in red.

(E) Sequence representation of the repeat mutations in KNL1-M_3 variants.

(F) As in (B), with the indicated KNL1-M_3 variants.

(G) Quantification of experiment in (F). Data are average of four experiments (+SD). BUB3-binding to GST-KNL1-M_3 was set to 1.

(H and I) Representative images (H) and quantification (I) of BUB1 kinetochore levels (corrected for LAP-KNL1 and CENP-C levels) in nocodazole-treated cells expressing $KNL1^{\Delta}$-M_3 and mutants thereof. Data are from 15 cells and representative of three experiments. Bars, 5 μm. Graph in (I) displays total kinetochore

(legend continued on next page)

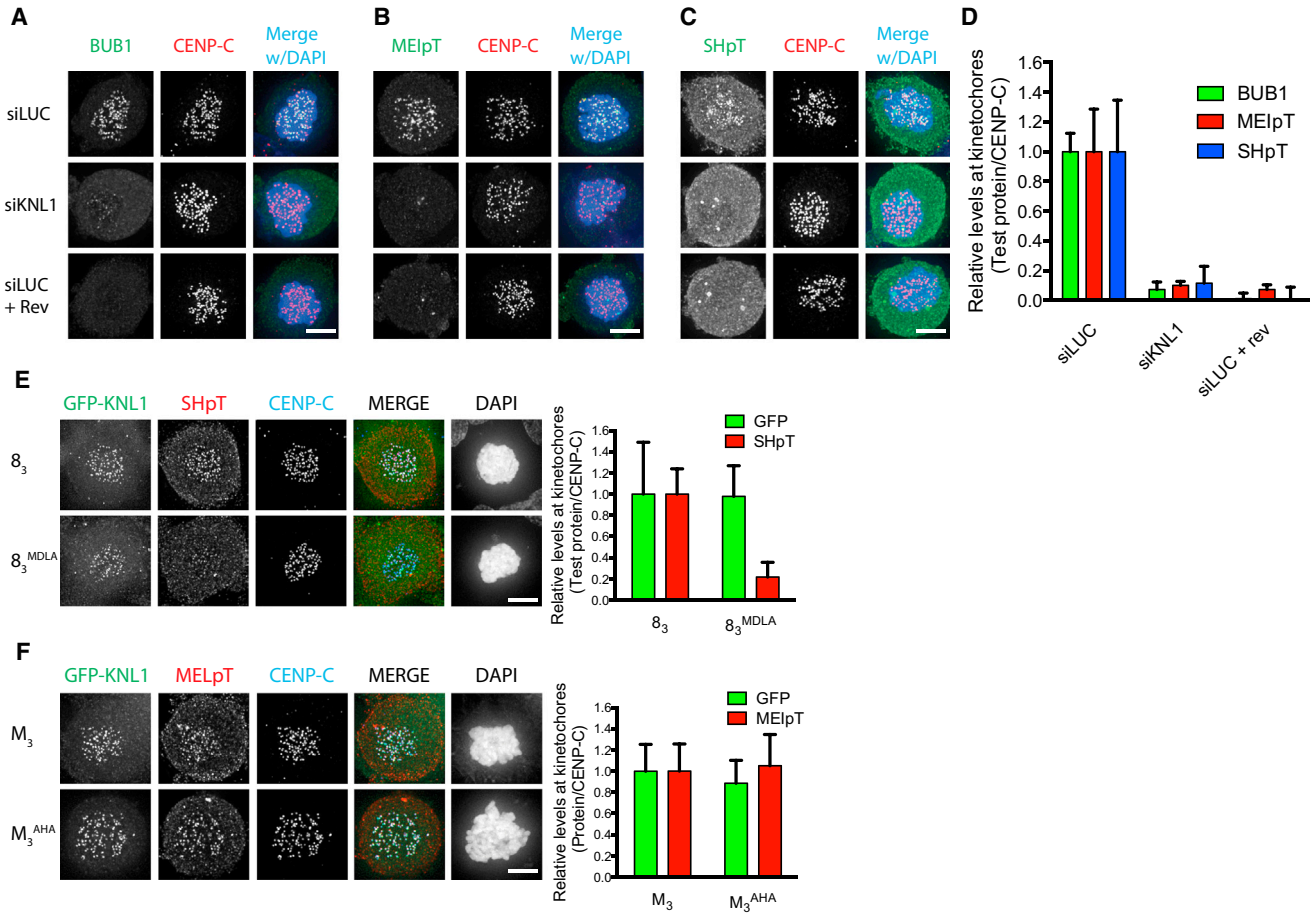

Figure 4. Phosphorylation of SHT Motifs by MPS1 Relies on Prior MELT Phosphorylation

(A–D) Representative images (A–C) and quantification (D) of BUB1, MElpT, or SHpT kinetochore levels in nocodazole-treated HeLa cells treated with siRNAs against luciferase (siLUC) or KNL1 (siKNL1) with or without 250 nM reversine. Bars, 5 μm. Graph in (D) displays total kinetochore signal intensities (+SD) of indicated antibodies as a ratio of CENP-C signals. Data are from 15 cells and representative of three experiments. Kinetochore levels in siLUC-treated cells were set to 1.

(E and F) Representative images (left) and quantification (right) of GFP kinetochore levels in nocodazole-treated cells expressing $KNL1^{\Delta}$-8_3 or $KNL1^{\Delta}$-M_3 and mutants thereof. Bars, 5 μm. Graphs display total kinetochore signal intensities (+SD) of GFP (LAP-KNL1) or phospho-antibodies corrected for CENP-C levels. Data are from 15 cells and representative of three experiments. Levels of GFP and phospho-antibodies were set to 1 in $KNL1^{\Delta}$-8_3- and $KNL1^{\Delta}$-M_3- expressing cells.

"MELT" motif (LEVTD). Structural analyses of BUB3/BUB1 with the extended human repeat may shed light on the exact requirements of repeat sequences for BUB3 binding. Such studies may also reveal the contribution of the TΩ motif. Its phosphorylation by MPS1 is not required, but the aromatic residue is essential (Vleugel et al., 2013).

Evolution of the KNL1-BUB3 Interfaces

In contrast to the relatively compact repeating module of budding yeast KNL1/Spc105, active repeats of human KNL1 are quite extensive and specified by the sequence DKTΦΦΩS[ED]x[ED]$_{2-3}$xxM[DE]ΦTKSHTΦxΦ. By in vitro reconstitution of the BUB-KNL1 complex, we show that the activities of individual repeats are directly related to their affinity for BUB1/BUB3 complexes and that the interface between BUB3 and KNL1 repeats is regulated through multisite phosphorylation. This includes phosphorylation of the vertebrate-specific SHT motif, which is likely to directly interact with an extended basic patch in human BUB3. One could envision that organisms with relatively simple kinetochore-microtubule attachments (like

signal intensities (+SD) of GFP and BUB1 as a ratio of CENP-C signals Levels of kinetochore LAP-KNL1 and BUB1 were set to 1 in $KNL1^{\Delta}$-M_3 expressing cells.

(J) Time-lapse analysis of Flp-in HeLa cells expressing LAP-KNL1 variants, treated with nocodazole and 250 nM reversine. Data (n = 40, representative of three independent experiments shown) indicate cumulative fraction of cells that exit from mitosis (as scored by cell morphology using DIC) at the indicated time after NEB.

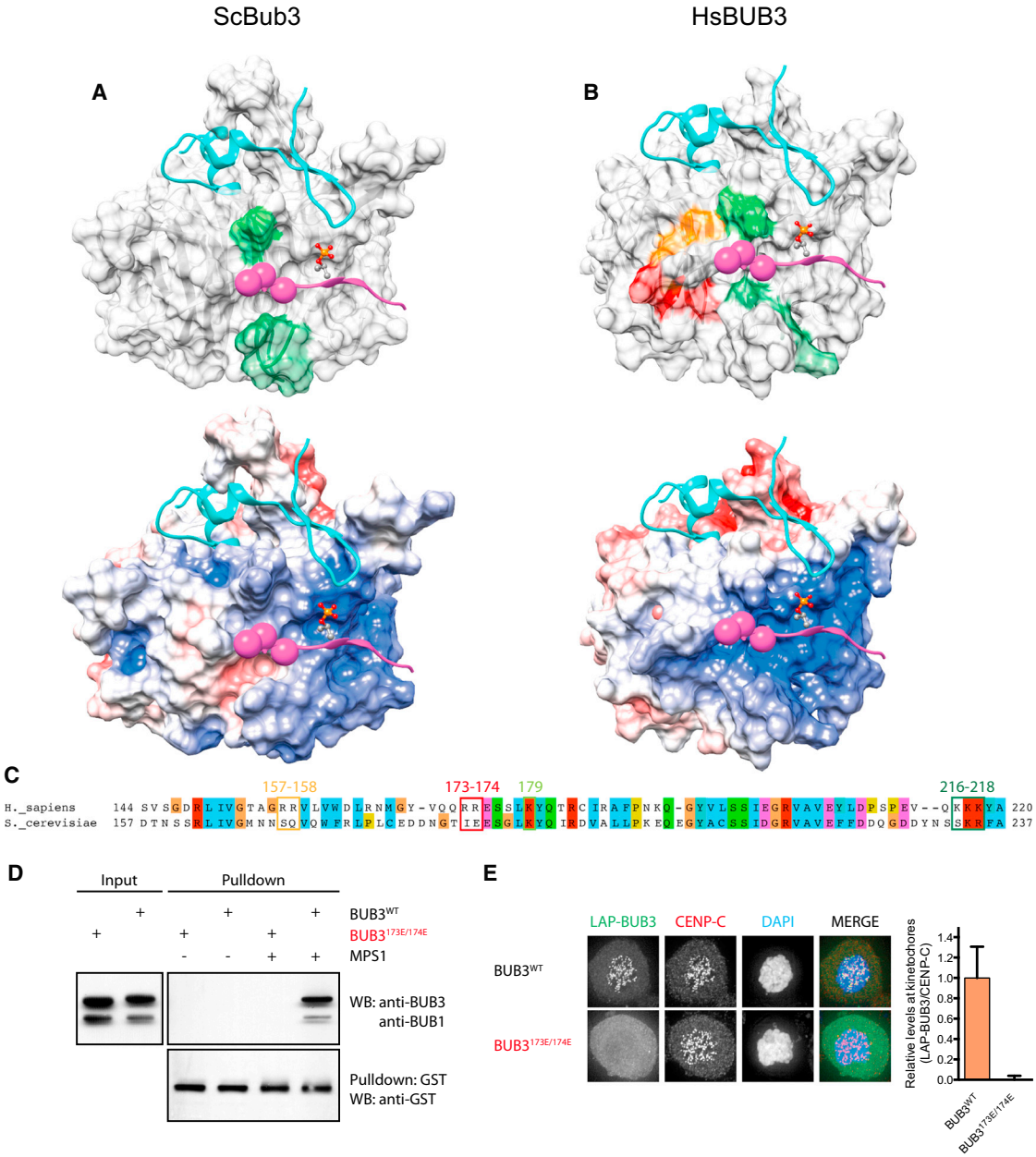

Figure 5. A Basic Patch on Human BUB3 Interacts with Phosphorylated SHT Motifs

(A and B) Structural representations of *S. cerevisiae* Bub3 (A: Primorac et al., 2013) or human BUB3 (B: homology model generated with I-TASSER; Roy et al., 2010) in complex with Bub1 (magenta) and a MEMpT peptide (purple), in which the pT (sticks) and position of the SHT motif (VFP in *S. cerevisiae*) (spheres) are indicated. Structures in lower panels are depictions of electrostatic surface potential as calculated by APBS (Baker et al., 2001) in Chimera (Pettersen et al., 2004), plotted from −7 kT/e (red) to +7 kT/e (blue). Colored patches in BUB3 in upper panels represent conserved basic residues (light and dark green) or basic only present in human BUB3 (red and orange).

(C) Sequence alignment of *H. sapiens* and *S. cerevisiae* BUB3 orthologs showing human-specific and shared basic residues. Colors of boxes correspond to colors in upper panels of (A) and (B).

(D) Immunoblots of BUB1, BUB3, and GST from in vitro binding assays of GST-KNL1 with His_6-$BUB1^{1-280}$/BUB3. GST-tagged KNL1-M_3 was pre-phosphorylated by 50 ng MPS1 (1 hr at 30°C), coupled to glutathione-agarose beads, and incubated with His_6-$BUB1^{1-280}$/BUB3 dimers ($BUB3^{WT}$ or $BUB3^{173E/174E}$) for 1 hr. Western blots are representative of three experiments.

(E) Representative images and quantification of GFP in nocodazole-treated HeLa cells expressing LAP-tagged BUB3 and mutants thereof. Bars, 5 μm. Graph displays total kinetochore signal intensities (+SD) of LAP-BUB3 over CENP-C. Data are from ten cells and representative of three experiments. Kinetochore levels in LAP-BUB3 wild-type expressing cells were set to 1.

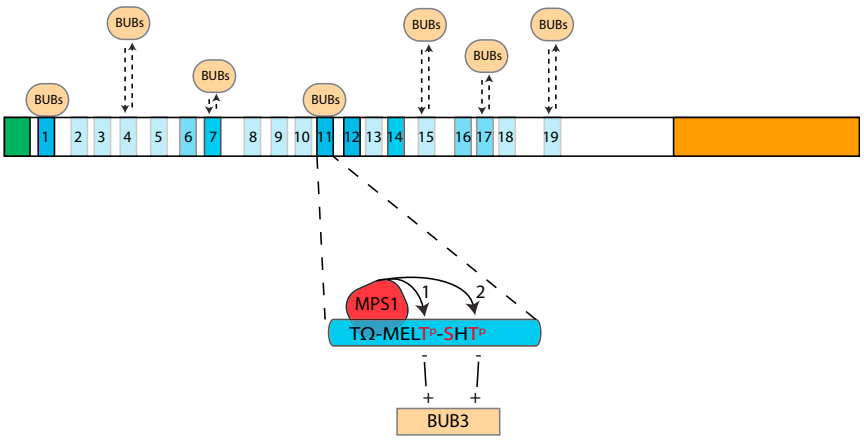

Figure 6. Model of MPS1-Mediated BUB1/BUB3 Kinetochore Recruitment

Schematic representation of KNL1 with individual repeats. Activity of repeats corresponds to color (dark blue is active, light blue is inactive) and to affinity for BUB protein complexes (indicated by arrow length). Combined activities result in decoration of KNL1 by BUB protein complexes in mitosis. Repeat activity relies on sequential phosphorylation of MELT and SHT motifs that synergize to provide acidic interaction surfaces (–) for basic patches (+) on BUB3.

budding yeast) require less kinetochore-localized Bub1 than those with more complicated kinetochore-microtubule interactions, which favors selection for KNL1 variants with fewer binding sites and ones with lower affinity. Budding yeast KNL1/Spc105 repeat sequences are indeed exceptionally simple, as they are among the shortest we identified in eukaryotes (Vleugel et al., 2013). The presence of a SHT motif in KNL1 orthologs co-occurs with the basic patch in BUB3 orthologs predicted to interact with SHpT, but not vice versa (not shown). An interesting hypothesis, therefore, is that extension of the KNL1/BUB3 interfaces by extensive and rapid alterations to KNL1 repeat sequences was enabled by a pre-existing basic surface of BUB3. From the perspective of co-evolution, it would be of interest to examine whether this basic surface contacts repeats of KNL1 homologs lacking the SHT motif or whether it contributes in ways unrelated to KNL1.

Human KNL1 contains 19 repeating sequences, of which many seem to have degenerated to a certain extent and only seven contribute significantly to BUB1 kinetochore recruitment. This suggests positive selection for maintaining a minimal number of active repeat sequences and raises the question of why repeats degenerate in the first place. Perhaps there is an adaptive conflict between certain evolutionary pressures that favor expansion of the number of repeats and the intolerance to having too many BUB1-binding sites at kinetochores. This could be examined by assessing chromosome segregation in cells expressing engineered KNL1 variants with an increased number of active repeats. Alternatively, demands for a certain amount of BUB molecules at kinetochores may vary periodically during evolution, requiring episodes of expansion and degeneration of the repeat array. Yet another scenario is that repeat expansion is "accidental" and due to, for instance, the nature of the KNL1 genomic locus. Degeneration would then be required to balance the amount of kinetochore BUB1 signaling. Given our results that single substitutions of either BUB3 or the repeats is sufficient to reduce their mutual affinity, repeat degeneration and subsequent survival of the lineage may be achieved relatively rapidly. It is of interest to note that KNL1 orthologs of some species do not (yet) contain significantly degenerated repeats (e.g., the lamprey fish and *Capsaspora owczarzaki*, a single-celled ophistokont) (Vleugel et al., 2013; E. Tromer and G.J.P.L.K., unpublished data). It will be interesting to examine if these repeats are equally functional or whether very subtle changes have nonetheless already altered their activity.

KNL1 Is Decorated with Multiple BUB1/BUB3 Dimers in Prometaphase

Our data indicate that at steady state in prometaphase, 6–7 BUB1 molecules bind to a single KNL1 molecule. Whereas SAC signaling requires less than 20% of normal BUB levels (Figure 1F), chromosome alignment requires near-maximal BUB1 levels, and the efficiency thereof directly correlates with the amount of BUB1/BUBR1 at kinetochores. We previously showed that low levels of BUB1 at kinetochores are sufficient for H2AT120 phosphorylation and by proxy for CPC localization (Vleugel et al., 2013). The need for high levels of BUB1 protein at kinetochores in order achieve efficient chromosome alignment is thus likely unrelated to BUB1 kinase activity and CPC localization. Instead, since BUBR1 kinetochore levels track those of BUB1 (Vleugel et al., 2013) (Figures S1A and S1B), we hypothesize that BUB1 mediates efficient chromosome alignment by promoting maximal BUBR1 kinetochore recruitment. BUBR1 controls the stability of kinetochore-microtubule attachments by binding the phosphatase PP2A-B56 that counters excessive Aurora B activity (Foley et al., 2011; Kruse et al., 2013; Suijkerbuijk et al., 2012b; Xu et al., 2013). Indirect regulation of localized PP2A-B56 activity by BUB1 may thus be the predominant role of BUB1 in chromosome alignment. Restoring PP2A-B56 at kinetochores with low BUB1 (for instance, in cells expressing KNL1-NC) will be required to examine this hypothesis.

EXPERIMENTAL PROCEDURES

Plasmids and Protein Purification

pCDNA5-LAP-KNL1^{FL} and KNL1$^{\Delta}$ constructs and cloning strategies are described in Vleugel et al., 2013. GST-KNL1 constructs were generated by insertion of the M_3 fragment and mutants thereof into the Xho1 site of pGEX-6P-1. GST-Knl1 constructs were expressed in BL21(DE3):DNAK for 4 hr at 20°C with 0.1 mM IPTG. Cell pellets were sonicated and lysed in lysis buffer (1x PBS solution, 0.1% Tween, 250 mM NaCl, 1 mM 2-mercaptoethanol, 1 mM DTT, and 10% glycerol). Proteins were purified using glutathione-agarose beads (Sigma) and eluted with 50 mM Tris-HCl (pH 8), 10 mM reduced

glutathione (Roche), and 75 mM KCl, followed by buffer exchange using desalting columns (Bio-Rad) in kinase buffer containing 12.5 mM Tris-HCl (pH 7.5), 35 mM KCl, 10 mM $MgCl_2$, 0.5 mM EGTA, 0.005% Triton-X, and 0.1 mM DTT. The His_6-$BUB1^{1-280}$/BUB3 construct (gift from Musacchio lab) and mutants thereof were co-expressed in Sf9 cells. Cell pellets were lysed in lysis buffer (50 mM Tris-HCl [pH 8], 300 mM NaCl, 5% glycerol, 1 mM β-mercaptoethanol) and purified using Ni-NTA beads (Bio-Rad). Proteins were eluted with 200 mM imidazole and buffer exchanged in 50 mM Tris-HCl (pH 7.5), 50 mM KCl, 0.05% Tween, 0.1 mM DTT, and 10% glycerol.

In Vitro Interaction Studies

GST-KNL1 constructs were pre-phosphorylated with 50 ng recombinant Mps1 kinase (Life Technologies) in kinase buffer with 500 μM ATP, 1 mM Na_3VO_4, 1 mM NaF, and 1 mM β-glycerophosphate for 1 hr at 30°C with constant shaking 1,200 rpm. Pre-phosphorylated proteins were incubated with 40 μl slurry of glutathione-agarose beads for 1 hr at room temperature and washed with washing buffer (50 mM Tris-HCl [pH 7.5], 150 mM KCl, 0.05% Tween, and 0.1 mM DTT). His_6-$BUB1^{1-280}$/BUB3 proteins were added to KNL1-bound beads and left incubating 1 hr shaking at room temperature in binding buffer (50 mM Tris-HCl [pH 7.5], 50 mM KCl, 0.05% Tween, 0.1 mM DTT, and 10% glycerol). The unbound proteins were washed 3× with washing buffer (50 mM Tris-HCl [pH 7.5], 150 mM KCl, 0.05% Tween, and 0.1 mM DTT). Beads were then boiled in 70 μl sample buffer and run on SDS-PAGE gel. Western blots were analyzed using LAS 4000 (GE Healthcare).

Cell Culture and Transfection

HeLa Flp-in cells were grown in DMEM containing 8% Tet-approved FBS (Clontech) supplemented with pen/strep (50 μg/ml), L-glutamine (2 mM), hygromycin (200 μg/ml), and blasticidin (4 μg/ml). Plasmids were transfected using FuGENE HD (Roche) according to the manufacturer's instructions. To generate stably integrated HeLa Flp-in cells, pCDNA5-constructs were co-transfected with Ogg44 recombinase in a 10:1 ratio (Vleugel et al., 2013). Constructs were expressed by addition of 1 μg/ml doxycycline for 24 hr. siKNL1 (CASC5#5; Dharmacon/J-015673-05; 5′-GCAUGUAUCUCUUAAGGAA-3′) and siBUB1 (5′-GAAUGUAAGCGUUCACGAA-3′) were transfected using Hiperfect (QIAGEN) at 20 nM for 2 days according to manufacturer's instructions.

Live-Cell Imaging

For live-cell imaging experiments, cells were transfected with 20 nM siRNA for 24 hr, after which cells were arrested in early S phase for 24 hr by addition of thymidine (2 mM), and expression was induced by addition of 1 μg/ml doxycycline. Subsequently, cells were released from thymidine for 8–10 hr and arrested in prometaphase by the addition of nocodazole (830 nM) with reversine (250 nM). Cells were imaged in a heated chamber (37°C and 5% CO_2) using a 20X/0.5NA UPLFLN objective on an Olympus IX-81 microscope, controlled by Cell-M software (Olympus). Images were acquired using a Hamamatsu ORCA-ER camera and processed using Cell-M software.

Immunofluorescence and Antibodies

Asynchronously growing cells were arrested in prometaphase by the addition of nocodazole (830 nM) for 1 hr. Cells plated on 12 mm coverslips were fixed (with 3.7% paraformaldehyde, 0.1% Triton X-100, 100 mM PIPES [pH 6.8], 1 mM $MgCl_2$, and 5 mM EGTA) for 5–10 min. Coverslips were washed with PBS and blocked with 3% BSA in PBS for 1 hr, incubated with primary antibodies for 16 hr at 4°C, washed with PBS containing 0.1% Triton X-100, and incubated with secondary antibodies for an additional hour at room temperature. Coverslips were then washed, incubated with DAPI for 2 min, and mounted using antifade (ProLong; Molecular Probes). All images were acquired on a deconvolution system (DeltaVision RT; Applied Precision) with a 100X/1.40NA U Plan S Apochromat objective (Olympus) using softWoRx software (Applied Precision). Images are maximum-intensity projections of deconvolved stacks. For quantification of immunostainings, all images of similarly stained experiments were acquired with identical illumination settings; cells expressing comparable levels of exogenous protein were selected for analysis and analyzed using ImageJ (National Institutes of Health). An ImageJ macro was used to threshold and select all centromeres and all chromosome areas (excluding centromeres) using the DAPI and CENP-C antibodies channels as described previously (Saurin et al., 2011). This was used to calculate the relative mean kinetochore intensity of various proteins ([centromeres − chromosome arm intensity (test protein)] / [centromeres − chromosome arm intensity (CENP-C or CREST)]).

Cells were stained using GFP-booster (ChromoTek), BUB1 (Bethyl), H2AT120P (ActiveMotif), CREST/anti-centromere antibodies (Cortex Biochem), and/or CENP-C (Sigma). Secondary antibodies were goat anti-human or goat anti-guinea pig Alexa Fluor 647 and goat anti-rabbit and anti-mouse Alexa Fluor 568 (Molecular Probes) for immunofluorescence experiments. Affinity-purified phospho-specific antibodies recognizing MElpT (13/17) and SHpT (8) were generated by rabbit injection with MElpTRSHTTALEC and MDLTESHpTSNLGSQC peptides, respectively (GenScript).

Relative Kinetochore Quantifications

HeLa FRT cells were treated with either siBUB1 or siKNL1, both of which diminished BUB1 kinetochore localization (Figure 1G; Figure S2B). In these cells we re-expressed LAP-BUB1 or LAP-KNL1, respectively, and we measured the increase of our BUB1-antibody staining over the GFP level in both LAP-BUB1 and LAP-KNL1 cells (Figures 1G and 1H, left graph). The right graph in Figure 1H shows a ratio of kinetochore levels of LAP-BUB1 over LAP-KNL1.

Mass Spectrometry

Cells were synchronized in mitosis by a 24 hr thymidine block, followed by overnight treatment with nocodazole. KNL1 expression was induced for 24 hr using doxycycline, and cells were harvested followed by immunoprecipitation and mass spectrometry. Cells were lysed at 4°C in hypertonic lysis buffer (500 mM NaCl, 50 mM Tris-HCl [pH 7.6], 0.1% sodium deoxycholate, and 1 mM DTT) including phosphatase inhibitors (1 mM sodium orthovanadate, 5 mM sodium fluoride, 1 mM β-glycerophosphate), sonicated, and LAP-KNL1 proteins were coupled to GFP-trap (ChromoTek) for 1 hr at 4°C. Purifications were washed three times with high-salt (2 M NaCl, 50 mM Tris-HCl [pH 7.6], 0.1% sodium deoxycholate, 1 mM DTT) and low-salt wash buffers (50 mM NaCl, 50 mM Tris-HCl [pH 7.6], 1 mM DTT) and subsequently eluted in 2 M urea, 50 mM Tris-HCl (pH 7.6), 5 mM IAA. Samples were loaded a C18 column and ran on a nano-LC system coupled to a mass spectrometer (LTQ-Orbitrap Velos; Thermo Fisher Scientific) via a nanoscale LC interface (Proxeon Biosystems, now Thermo Fisher Scientific), as described in Suijkerbuijk et al., 2012a.

SUPPLEMENTAL INFORMATION

Supplemental Information includes five figures and one table and can be found with this article online at http://dx.doi.org/10.1016/j.molcel.2014.12.036.

ACKNOWLEDGMENTS

We thank the Kops and Lens labs for discussions and A. Musacchio for sharing reagents. This work was supported by grants from the Netherlands Organisation for Scientific Research (NWO-Vici 865.12.004), from the European Research Council (ERC-StG KINSIGN), and from TiPharma (T3-503).

Received: August 20, 2014
Revised: November 8, 2014
Accepted: December 22, 2014
Published: February 5, 2015

REFERENCES

Baker, N.A., Sept, D., Joseph, S., Holst, M.J., and McCammon, J.A. (2001). Electrostatics of nanosystems: application to microtubules and the ribosome. Proc. Natl. Acad. Sci. USA *98*, 10037–10041.

Cheeseman, I.M., and Desai, A. (2008). Molecular architecture of the kinetochore-microtubule interface. Nat. Rev. Mol. Cell Biol. *9*, 33–46.

Cheeseman, I.M., Chappie, J.S., Wilson-Kubalek, E.M., and Desai, A. (2006). The conserved KMN network constitutes the core microtubule-binding site of the kinetochore. Cell *127*, 983–997.

Dephoure, N., Zhou, C., Villén, J., Beausoleil, S.A., Bakalarski, C.E., Elledge, S.J., and Gygi, S.P. (2008). A quantitative atlas of mitotic phosphorylation. Proc. Natl. Acad. Sci. USA *105*, 10762–10767.

Dou, Z., von Schubert, C., Körner, R., Santamaria, A., Elowe, S., and Nigg, E.A. (2011). Quantitative mass spectrometry analysis reveals similar substrate consensus motif for human Mps1 kinase and Plk1. PLoS ONE *6*, e18793.

Foley, E.A., and Kapoor, T.M. (2013). Microtubule attachment and spindle assembly checkpoint signalling at the kinetochore. Nat. Rev. Mol. Cell Biol. *14*, 25–37.

Foley, E.A., Maldonado, M., and Kapoor, T.M. (2011). Formation of stable attachments between kinetochores and microtubules depends on the B56-PP2A phosphatase. Nat. Cell Biol. *13*, 1265–1271.

Grosstessner-Hain, K., Hegemann, B., Novatchkova, M., Rameseder, J., Joughin, B.A., Hudecz, O., Roitinger, E., Pichler, P., Kraut, N., Yaffe, M.B., et al. (2011). Quantitative phospho-proteomics to investigate the polo-like kinase 1-dependent phospho-proteome. Mol. Cell. Proteomics *10*, 008540.

Hegemann, B., Hutchins, J.R., Hudecz, O., Novatchkova, M., Rameseder, J., Sykora, M.M., Liu, S., Mazanek, M., Lénárt, P., Hériché, J.K., et al. (2011). Systematic phosphorylation analysis of human mitotic protein complexes. Sci. Signal. *4*, rs12.

Hennrich, M.L., Marino, F., Groenewold, V., Kops, G.J., Mohammed, S., and Heck, A.J. (2013). Universal quantitative kinase assay based on diagonal SCX chromatography and stable isotope dimethyl labeling provides high-definition kinase consensus motifs for PKA and human Mps1. J. Proteome Res. *12*, 2214–2224.

Hoyt, M.A., Totis, L., and Roberts, B.T. (1991). S. cerevisiae genes required for cell cycle arrest in response to loss of microtubule function. Cell *66*, 507–517.

Jelluma, N., Brenkman, A.B., van den Broek, N.J., Cruijsen, C.W., van Osch, M.H., Lens, S.M., Medema, R.H., and Kops, G.J. (2008). Mps1 phosphorylates Borealin to control Aurora B activity and chromosome alignment. Cell *132*, 233–246.

Kawashima, S.A., Yamagishi, Y., Honda, T., Ishiguro, K.I., and Watanabe, Y. (2009). Phosphorylation of H2A by Bub1 prevents chromosomal instability through localizing shugoshin. Science *327*, 172–177.

Kitajima, T.S., Hauf, S., Ohsugi, M., Yamamoto, T., and Watanabe, Y. (2005). Human Bub1 defines the persistent cohesion site along the mitotic chromosome by affecting Shugoshin localization. Curr. Biol. *15*, 353–359.

Kiyomitsu, T., Obuse, C., and Yanagida, M. (2007). Human Blinkin/AF15q14 is required for chromosome alignment and the mitotic checkpoint through direct interaction with Bub1 and BubR1. Dev. Cell *13*, 663–676.

Krenn, V., Overlack, K., Primorac, I., van Gerwen, S., and Musacchio, A. (2014). KI motifs of human Knl1 enhance assembly of comprehensive spindle checkpoint complexes around MELT repeats. Curr. Biol. *24*, 29–39.

Kruse, T., Zhang, G., Larsen, M.S., Lischetti, T., Streicher, W., Kragh Nielsen, T., Bjørn, S.P., and Nilsson, J. (2013). Direct binding between BubR1 and B56-PP2A phosphatase complexes regulate mitotic progression. J. Cell Sci. *126*, 1086–1092.

Larsen, N.A., Al-Bassam, J., Wei, R.R., and Harrison, S.C. (2007). Structural analysis of Bub3 interactions in the mitotic spindle checkpoint. Proc. Natl. Acad. Sci. USA *104*, 1201–1206.

Li, R., and Murray, A.W. (1991). Feedback control of mitosis on budding yeast. Cell *66*, 519–531.

Liu, D., Vleugel, M., Backer, C.B., Hori, T., Fukagawa, T., Cheeseman, I.M., and Lampson, M.A. (2010). Regulated targeting of protein phosphatase 1 to the outer kinetochore by KNL1 opposes Aurora B kinase. J. Cell Biol. *188*, 809–820.

London, N., Ceto, S., Ranish, J.A., and Biggins, S. (2012). Phosphoregulation of Spc105 by Mps1 and PP1 regulates Bub1 localization to kinetochores. Curr. Biol. *22*, 900–906.

Meadows, J.C., Shepperd, L.A., Vanoosthuyse, V., Lancaster, T.C., Sochaj, A.M., Buttrick, G.J., Hardwick, K.G., and Millar, J.B. (2011). Spindle checkpoint silencing requires association of PP1 to both Spc7 and kinesin-8 motors. Dev. Cell *20*, 739–750.

Nijenhuis, W., Vallardi, G., Teixeira, A., Kops, G.J.P.L., and Saurin, A. (2014). Negative feedback at kinetochores underlies a responsive spindle checkpoint signal. Nat. Cell Biol. *16*, 1257–1264.

Petrovic, A., Mosalaganti, S., Keller, J., Mattiuzzo, M., Overlack, K., Krenn, V., De Antoni, A., Wohlgemuth, S., Cecatiello, V., Pasqualato, S., et al. (2014). Modular assembly of RWD domains on the Mis12 complex underlies outer kinetochore organization. Mol. Cell *53*, 591–605.

Pettersen, E.F., Goddard, T.D., Huang, C.C., Couch, G.S., Greenblatt, D.M., Meng, E.C., and Ferrin, T.E. (2004). UCSF Chimera—a visualization system for exploratory research and analysis. J. Comput. Chem. *25*, 1605–1612.

Primorac, I., Weir, J.R., Chiroli, E., Gross, F., Hoffmann, I., van Gerwen, S., Ciliberto, A., and Musacchio, A. (2013). Bub3 reads phosphorylated MELT repeats to promote spindle assembly checkpoint signaling. eLife *2*, e01030.

Rosenberg, J.S., Cross, F.R., and Funabiki, H. (2011). KNL1/Spc105 recruits PP1 to silence the spindle assembly checkpoint. Curr. Biol. *21*, 942–947.

Roy, A., Kucukural, A., and Zhang, Y. (2010). I-TASSER: a unified platform for automated protein structure and function prediction. Nat. Protoc. *5*, 725–738.

Sacristan, C., and Kops, G.J.P.L. (2014). Joined at the hip: kinetochores, microtubules, and spindle assembly checkpoint signaling. Trends Cell Biol. *25*, 21–28.

Santaguida, S., Vernieri, C., Villa, F., Ciliberto, A., and Musacchio, A. (2011). Evidence that Aurora B is implicated in spindle checkpoint signalling independently of error correction. EMBO J. *30*, 1508–1519.

Saurin, A.T., van der Waal, M.S., Medema, R.H., Lens, S.M., and Kops, G.J. (2011). Aurora B potentiates Mps1 activation to ensure rapid checkpoint establishment at the onset of mitosis. Nat. Commun. *2*, 316.

Shepperd, L.A., Meadows, J.C., Sochaj, A.M., Lancaster, T.C., Zou, J., Buttrick, G.J., Rappsilber, J., Hardwick, K.G., and Millar, J.B. (2012). Phosphodependent recruitment of Bub1 and Bub3 to Spc7/KNL1 by Mph1 kinase maintains the spindle checkpoint. Curr. Biol. *22*, 891–899.

Suijkerbuijk, S.J., van Dam, T.J., Karagöz, G.E., von Castelmur, E., Hubner, N.C., Duarte, A.M., Vleugel, M., Perrakis, A., Rüdiger, S.G., Snel, B., and Kops, G.J. (2012a). The vertebrate mitotic checkpoint protein BUBR1 is an unusual pseudokinase. Dev. Cell *22*, 1321–1329.

Suijkerbuijk, S.J., Vleugel, M., Teixeira, A., and Kops, G.J. (2012b). Integration of kinase and phosphatase activities by BUBR1 ensures formation of stable kinetochore-microtubule attachments. Dev. Cell *23*, 745–755.

Taylor, S.S., Ha, E., and McKeon, F. (1998). The human homologue of Bub3 is required for kinetochore localization of Bub1 and a Mad3/Bub1-related protein kinase. J. Cell Biol. *142*, 1–11.

Vleugel, M., Hoogendoorn, E., Snel, B., and Kops, G.J. (2012). Evolution and function of the mitotic checkpoint. Dev. Cell *23*, 239–250.

Vleugel, M., Tromer, E., Omerzu, M., Groenewold, V., Nijenhuis, W., Snel, B., and Kops, G.J. (2013). Arrayed BUB recruitment modules in the kinetochore scaffold KNL1 promote accurate chromosome segregation. J. Cell Biol. *203*, 943–955.

Welburn, J.P., Vleugel, M., Liu, D., Yates, J.R., 3rd, Lampson, M.A., Fukagawa, T., and Cheeseman, I.M. (2010). Aurora B phosphorylates spatially distinct targets to differentially regulate the kinetochore-microtubule interface. Mol. Cell *38*, 383–392.

Xu, P., Raetz, E.A., Kitagawa, M., Virshup, D.M., and Lee, S.H. (2013). BUBR1 recruits PP2A via the B56 family of targeting subunits to promote chromosome congression. Biol. Open *2*, 479–486.

Yamagishi, Y., Yang, C.H., Tanno, Y., and Watanabe, Y. (2012). MPS1/Mph1 phosphorylates the kinetochore protein KNL1/Spc7 to recruit SAC components. Nat. Cell Biol. *14*, 746–752.

Zhang, G., Lischetti, T., and Nilsson, J. (2014). A minimal number of MELT repeats supports all the functions of KNL1 in chromosome segregation. J. Cell Sci. *127*, 871–884.